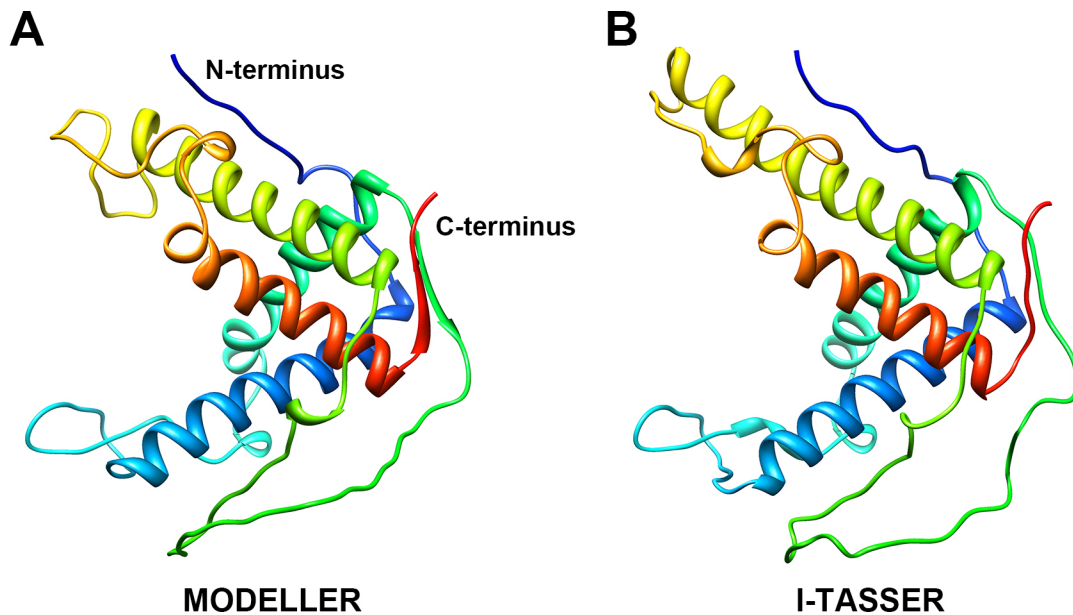


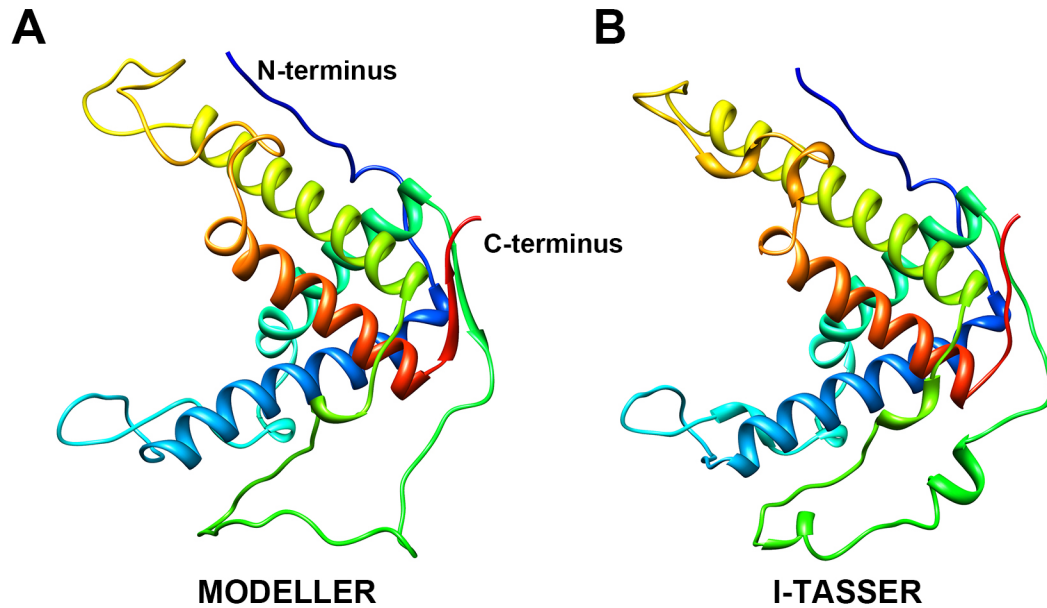
## Supplemental Information

Supplemental Figure S1. Comparison of pseudo-atomic models of RyR1 fragment (residues 850-1,056).



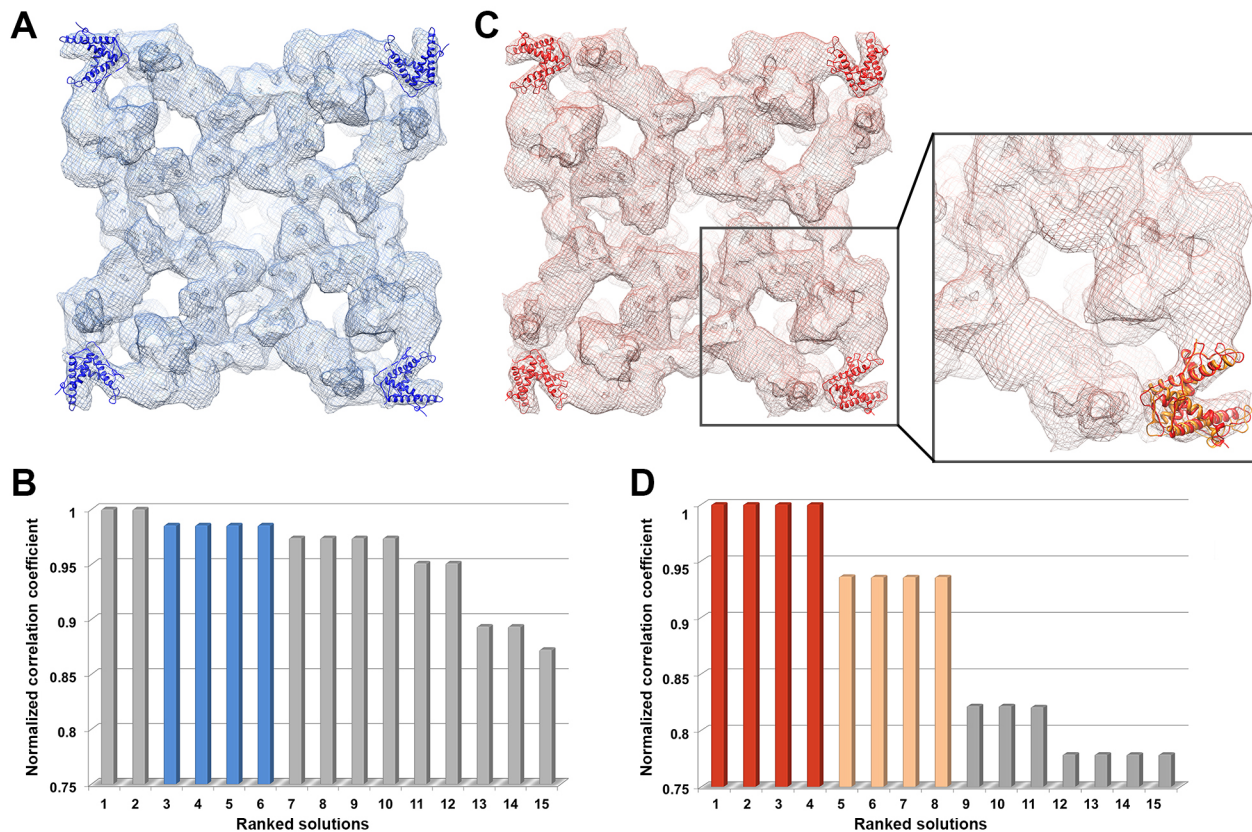
Pseudo-atomic models of rabbit RyR1 fragment (residues 850-1,056) generated using MODELLER (A) and I-TASSER (B). The ribbon diagram is colored in a rainbow from blue to red mapping the sequence from N- to C-terminus.

**Supplemental Figure S2. Comparison of pseudo-atomic models of RyR2 fragment (residues 861-1,067).**



Pseudo-atomic models of mouse RyR2 fragment (residues 861-1,067) generated using MODELLER (A) and I-TASSER (B). The ribbon diagram is colored in a rainbow from blue to red mapping the sequence from N- to C-terminus.

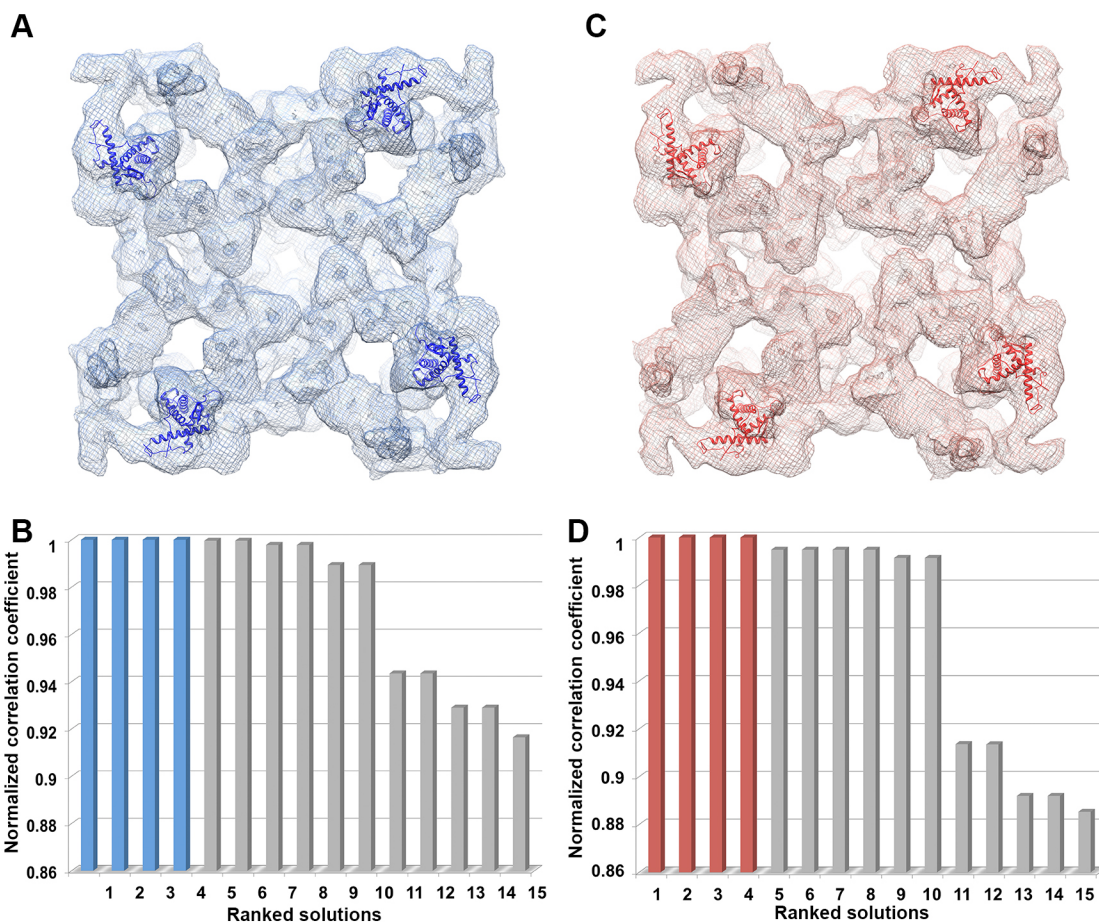
### Supplemental Figure S3. Docking crystal structure 3RQR into cryo-EM maps of RyR1.



(A). Crystal structure 3RQR (shown as blue ribbons) docked into the cryo-EM map of closed conformation RyR1 (EMDB 1606, shown in blue mesh). (B). Top ranked docking solutions of 3RQR in the closed state RyR1, solutions ranked 3 - 6 (blue bars) are the four positions shown as blue ribbons in panel A. Solutions ranked 1 and 2 dock in the center of cytoplasmic assembly and do not show the 4 repeats expected in the tetrameric structure of RyR. (C) 3RQR (shown in red or yellow ribbons) docked into the cryo-EM map of open conformation RyR1

(EMDB 1607, shown in red mesh), The close-up view shows two docking positions that are pseudo-mirrored. (D) Top ranked docking solutions of 3RQR in the open state RyR1, solutions ranked 1 - 4 (red bars) are the four positions shown as red ribbons in panel C, and solutions ranked 5 - 8 (yellow bars) are the positions shown as yellow ribbons.

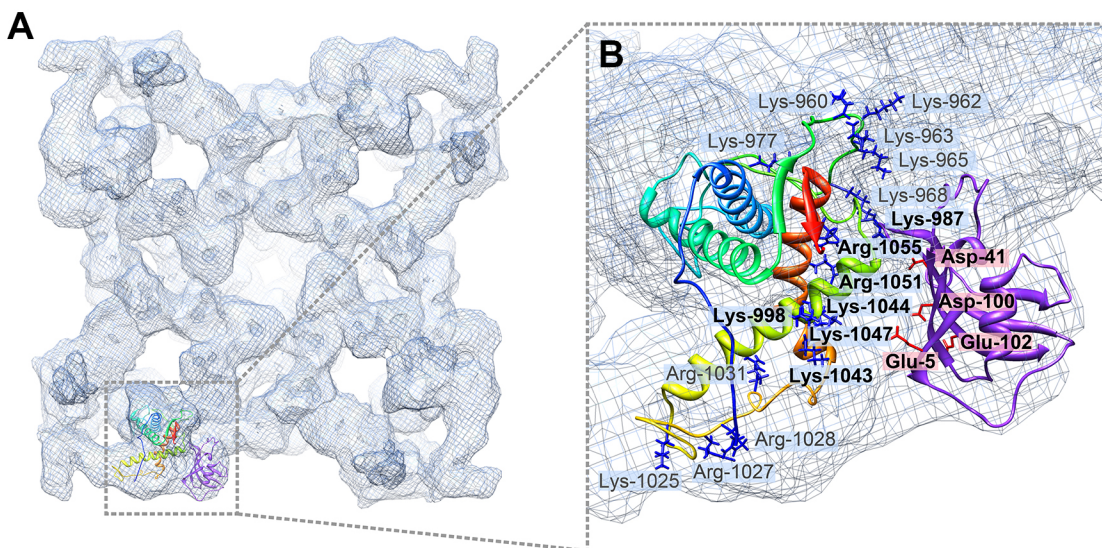
**Supplemental Figure S4. Docking pseudo-atomic model of RyR2 fragment (residues 861-1,067) into cryo-EM maps of RyR1.**



(A). Pseudo-atomic model of RyR2 fragment (residues 861-1,067, shown as blue ribbons) docked into the cryo-EM map of closed conformation RyR1 (EMDB 1606, shown in blue mesh). (B). Top ranked docking solutions in the closed state RyR1, solutions ranked 1 - 4 (blue bars) are the four positions shown as blue ribbons in panel A. (C) Pseudo-atomic model of RyR2 fragment (residues 861-1,067, shown as red ribbons) docked into the cryo-EM map of open conformation

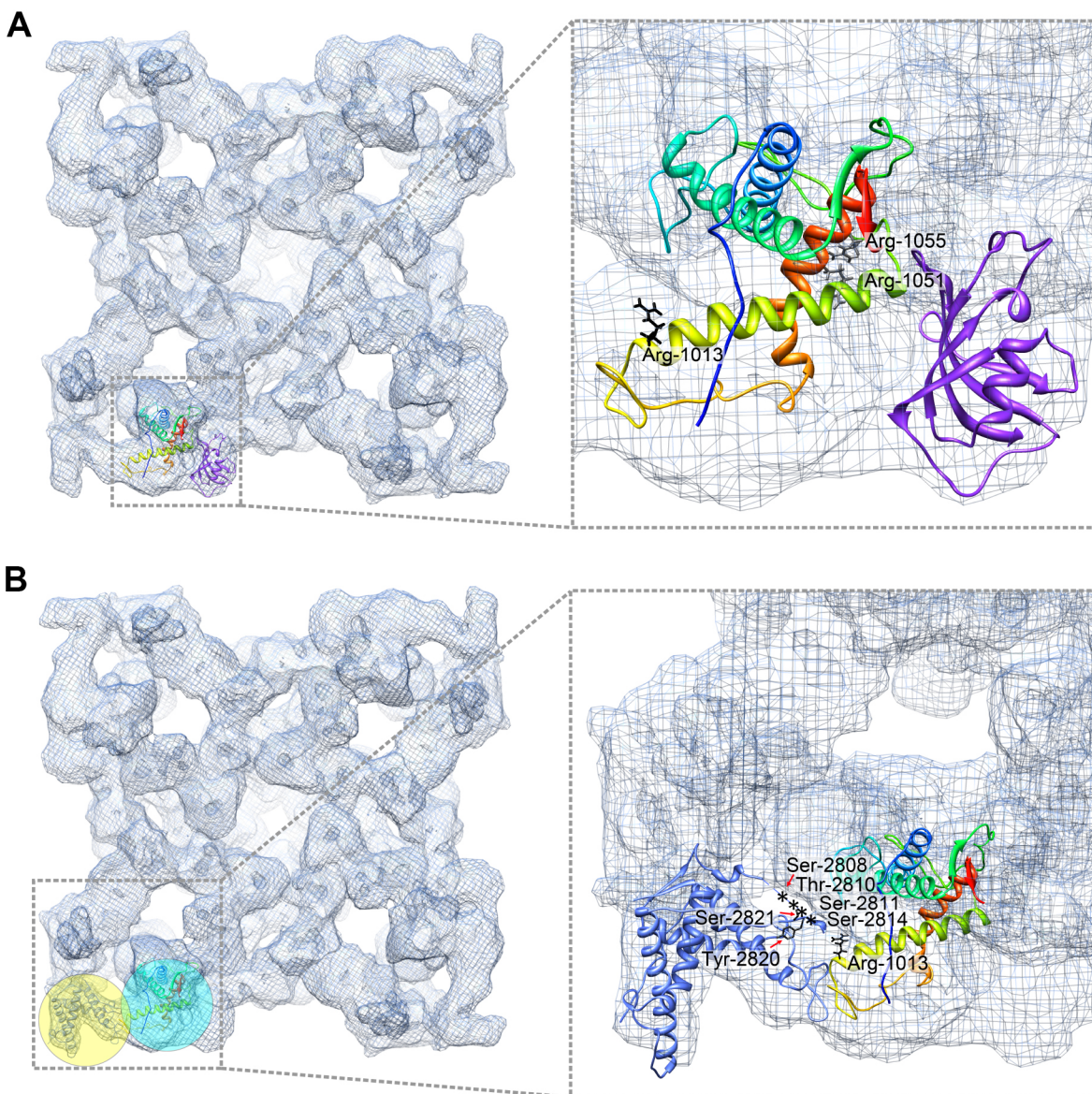
RyR1 (EMDB 1607, shown in red mesh). (D) Top ranked docking solutions in the open state RyR1, solutions ranked 1 - 4 (red bars) are the positions shown as red ribbons in panel C.

**Supplemental Figure S5. Interaction between docked pseudo-atomic model of RyR2 fragment (residues 861-1,067) and docked FKBP12.6.**



(A). Flexibly fitted pseudo-atomic model of RyR2 fragment (residues 861-1,067) and the rigid-body docked FKBP12.6 crystal structure in the closed conformation cryo-EM map of RyR1. For clarity, the docked structures are only shown in one subunit. (B) Close-up view of interface between RyR2 fragment (residues 861-1,067) and FKBP12.6. Positively charged residues in RyR2 are depicted as blue stick structures, and negatively charged residues in FKBP12.6 are indicated as red stick structures. Residues with number in bold are located at the direct interface.

**Supplemental Figure S6. Mapping disease-causing mutations in pseudo-atomic model of RyR2 fragment (residues 861-1,067).**



(A). The flexibly fitted pseudo-atomic model of RyR2 fragment (residues 861-1,067) with disease-related residues depicted as black stick structures. Two residues, Arg1051 and Arg1055, are located in helix 4 (orange-red), which are at the RyR2/FKBP12.6 interface, potentially mediating the RyR-FKBP interaction.



(B). One residue Arg1013 is located at the interface between domains 9 (cyan sphere) and domain 10 (yellow sphere), where the pseudo-atomic model interacts with the docked crystal structure of the phosphorylation domain in RyR2 shown as blue ribbon (PDB entry code 4ETV, residues 2,699-2,904). Residues in human RyR2 phosphorylation loop that can be phosphorylated by PKA or CaMKII are depicted as back stick structures or asterisks in the unstructured loop.

**Supplemental Table S1. Optimization of MDFF protocols.**

Cryo-EM maps	Optimized pseudo-atomic model	MDFF protocol				Structure prediction program
		Stimulation length		Initial CCC	Final CCC	
<b>EMD entry code 1606</b>	rabbit RyR1 a.a. 850~1056	50ps	200+5000	0.66607	0.697425	MODELLER
		50ps	200+5000	0.66005	0.701608	I-TASSER
	mouse RyR2 a.a. 861~1067	100ps	200+10000	0.65936	0.695293	MODELLER
		100ps	200+20000	0.606782	0.679436	I-TASSER
<b>EMD entry code 1607</b>	rabbit RyR1 a.a. 850~1056	1000ps	200+20000	0.638118	0.687611	MODELLER
		50ps	200+5000	0.637772	0.681986	I-TASSER
	mouse RyR2 a.a. 861~1067	100ps	200+10000	0.650641	0.688346	MODELLER
		50ps	200+5000	0.631817	0.677015	I-TASSER

Optimization of molecular dynamics flexible fitting (MDFF) protocol for flexibly fitting pseudo-atomic models for RyR1 fragment (residues 850-1,056) and RyR2 fragment (residues 861-1,067) into RyR1 cryo-EM maps in closed (EMDB 1606) and open (EMDB 1607) conformations. The MDFF protocol column shows the simulation steps (first column) and the energy minimization steps (second column). The initial and final CCC (cross-correlation coefficient) columns refer to the CCC before and after MDFF optimization, respectively.